applied sciences

MDPI

Article

Properties of Insulation-Type Green Composite Panels Manufactured from Recycled Cardboard

Mohammad Hassan Mazaherifar [1], Salim Hiziroglu [2], Luminita Maria Brenci [1,*] and Camelia Cosereanu [1]

[1] Faculty of Furniture Design and Wood Engineering, Transilvania University of Brasov, B-dul Eroilor nr. 29, 500036 Brasov, Romania; mohammad.mazaherifar@unitbv.ro (M.H.M.); cboieriu@unitbv.ro (C.C.)
[2] Department of Natural Resource Ecology and Management, Oklahoma State University, Stillwater, OK 74078-6013, USA; salim.hiziroglu@okstate.edu
* Correspondence: brenlu@unitbv.ro

Abstract

This study investigates the influence of two processing methods, namely wet and dry, on the structural, physical, mechanical, and acoustic performance of green lignocellulosic fiber-based composite panels. A comprehensive evaluation was carried out to compare the vertical density profile, affinity to water, thermal insulation and sound absorption, microstructural features, and mechanical performance of two types of experimental panels. The dry-processed samples exhibited 24% more prominent vertical density profile and superior dimensional stability, with lower thickness swelling (TS) and water absorption (WA) due to their more compact fiber arrangement compared to those of the specimens made using the wet process. However, the wet-processed panel demonstrated significantly enhanced mechanical properties, including 36% higher modulus of elasticity (MOE), 61% modulus of rupture (MOR), and 67% internal bonding strength (IB). Such findings could be attributed to their increased fibrillation and improved inter-fiber bonding compared with those of the panels made using the dry process. The thermal conductivity values of the wet- and dry-processed panels were found to be 0.053 W/mK and 0.057 W/mK, respectively. Acoustic analysis of the samples revealed that while the dry-processed panel slightly outperformed in terms of low-frequency sound absorption, the wet-processed panel exhibited superior high-frequency absorption, particularly when perforations were introduced. Microscopic examination of the samples confirmed that wet processing produced a more homogenous and fibrillated microstructure, correlating well with the observed enhancements in mechanical and acoustic performance. In conclusion, it can be stated that the processing strategies of such panels could be applied for diverse engineering applications, including thermal insulation, acoustic damping, and sustainable structural materials.

Keywords: recycled cardboard; green composite panels; lignocellulosic fiber; acoustic absorption behavior; mechanical properties

Academic Editor: Asterios Bakolas

Received: 3 September 2025
Revised: 19 September 2025
Accepted: 23 September 2025
Published: 24 September 2025

Citation: Mazaherifar, M.H.; Hiziroglu, S.; Brenci, L.M.; Cosereanu, C. Properties of Insulation-Type Green Composite Panels Manufactured from Recycled Cardboard. *Appl. Sci.* **2025**, *15*, 10378. https://doi.org/10.3390/app151910378

1. Introduction

Improving the energy efficiency of buildings has emerged as a critical strategy for mitigating global energy consumption and reducing greenhouse gas emissions. The building sector alone accounts for a substantial portion of worldwide energy use, primarily due to heating, cooling, and ventilation requirements. To address this issue, passive design approaches, particularly thermal and sound insulation, have gained prominence as cost-effective and sustainable solutions for minimizing energy losses and enhancing indoor

comfort [1]. Generally, insulating materials offer benefits such as low density, a large specific surface area, and adaptable raw material profiles [2,3].

Thermal and sound insulation play a pivotal role in maintaining a stable indoor environment by reducing heat transfer and sound transmission through the building envelope. Conventional insulation materials encompass a range of inorganic and synthetic options, including fiberglass, vermiculite, expanded polystyrene (EPS), and polyurethane foams [4–6]. These materials exhibit favorable thermal performance. However, their production often relies on non-renewable resources, involving energy-intensive manufacturing processes, creating challenges for end-of-life disposal due to poor biodegradability and toxic emissions [7–9].

Consequently, there is a growing impetus to explore environmentally benign alternatives that align with the principles of sustainable development and the circular economy. Research has increasingly focused on insulation materials derived from renewable, biodegradable, and recycled sources. Lignocellulosic biomass, including agricultural residues, wood fibers, and recycled paper products, has shown promise as a sustainable insulation feedstock due to its low cost, high availability, and favorable thermal and mechanical properties [2,9]. Among recycled materials, paper and cardboard stand out as particularly attractive, given their high cellulose content, biodegradability, and widespread post-consumer availability. Furthermore, it results in optimizing resource consumption due to the utilization of recycled materials [1].

Corrugated cardboard, a primary component of global packaging systems, is largely composed of recycled cellulose fibers and exhibits excellent mechanical strength, low density, and good recyclability [10]. Globally, more than 50 million metric tons of corrugated cardboard are produced annually, with recycling rates approaching 90% in many countries [11]. While such a resource can be recycled up to 25 times [12], fiber degradation and environmental burdens associated with cardboard manufacturing and waste disposal, such as high water and energy consumption and methane emissions from landfills, remain persistent challenges [13,14].

Valorizing recycled cardboard into high-performance insulation composites offers a compelling solution to extend the lifecycle of paper-based materials while addressing environmental concerns. Previous studies have demonstrated the integration of recycled cardboard into structural components such as fiber-reinforced concrete [15], sandwich beams manufactured by using cardboard in the core [16,17], and gypsum-based insulation boards [18]. However, applications in thermal and acoustic insulation remain underexplored, particularly using low-energy, non-toxic manufacturing methods.

One emerging approach involves combining recycled cardboard fibers with foaming and leavening agents, such as sodium bicarbonate and yeast, to create lightweight, porous insulation composites. These agents promote gas formation during processing, resulting in materials with low thermal conductivity and enhanced sound absorption. In a recent study, eco-panels made from recycled cardboard, sodium bicarbonate, and baking powder achieved a thermal conductivity coefficient near 0.05 W/mK and sound absorption coefficient of 0.85 at 700 Hz [19].

However, cellulose can also serve as the sole structural component for producing lightweight, porous materials without the need for an additional supporting matrix. Cellulose-based foams are commonly fabricated via a two-step wet processing route. In the first stage, an aqueous fiber suspension is transformed into a wet foam by introducing gas bubbles through mechanical agitation or air sparging, thereby generating a highly aerated structure. The second stage involves removing the liquid phase, typically achieved through freeze-drying, evaporation, or supercritical drying, to preserve the porous architecture and achieve the desired density and structural stability [20,21].

Despite these promising outcomes, there is still limited information on the characteristics of such panels, and further research is needed to optimize the composition, processing parameters, and performance characteristics of cardboard-based insulation materials to meet regulatory and functional standards. In particular, understanding how foaming agents interact with recycled fibers to influence porosity, mechanical integrity, and moisture resistance is important for the practical use of these materials.

Therefore, the objective of the present study is to develop lightweight, eco-friendly insulation-type composites by repurposing recycled corrugated cardboard and incorporating commonly available foaming and leavening agents. The research focuses on evaluating the thermal, acoustic, physical, and mechanical properties of the proposed composites through a simplified, sustainable manufacturing process. The data and information from the results of this work are expected to provide us with a better understanding of circular, biodegradable insulation alternatives with the potential to reduce dependence on conventional inorganic and synthetic materials in the construction industry.

2. Materials and Methods

2.1. Preparation of the Raw Materials

Unprinted cardboard was obtained from the recycling bin of a local store. Two distinct wet and dry defibration methods were employed to process the material. For the wet defibration method, the cardboard was first manually torn into smaller fragments before being immersed in water for two hours to facilitate softening. Once sufficiently saturated, the material was mechanically defibrated using a high-speed blender operating at 9000 rpm for one minute. A cardboard-to-water ratio of 1:12 by weight was maintained throughout this process. In the dry defibration method, the unprinted cardboard was also manually pre-torn into small fragments. Subsequently, the material was processed using a mechanical impact mill operating at approximately 1500 rpm to achieve fiber separation. The physical [22], chemical [23,24], and morphological [25,26] characteristics of the fibers defibrated from the cardboard are displayed in Table 1.

Table 1. Properties of cardboard fibers.

	Physical Properties	**Morphological Properties**			**Chemical Properties**				
Cellulose Fibers	Density (kg/m^3)	Length (µm)	Width (µm)	Diameter (µm)	Cellulose %	Hemicellulose %	Lignin %	Ash %	Additives %
	1500–1600	192	53	10–50	40–80	5–15	10–15	15	15

To manufacture the experimental panels, both wet- and dry-defibrated fibers were used in a formulation comprising four components: 500 g of processed unprinted cardboard, 2.5 L of water, sodium bicarbonate 12% by weight of the total mixture, and yeast 8% by weight of the total mixture.

2.2. Manufacturing of the Panels

Two types of green composite samples were manufactured under controlled laboratory conditions using defibrated fibers derived from unprinted cardboard. These fibers, as primary material, were prepared for both dry and wet defibration techniques, as illustrated in Figures 1a and 1b, respectively. Prior to shaping, sodium bicarbonate and yeast were incorporated into the mixture to aid in the expansion and structuring of the composite matrix. The prepared mixtures were then poured onto mold-lined trays covered with baking paper, as depicted in Figure 1c. Manufacturing was carried out by baking in an oven for 15 h at a temperature of 150 °C. Following thermal treatment, the composites were cooled off at ambient temperature, as shown in Figure 1d.

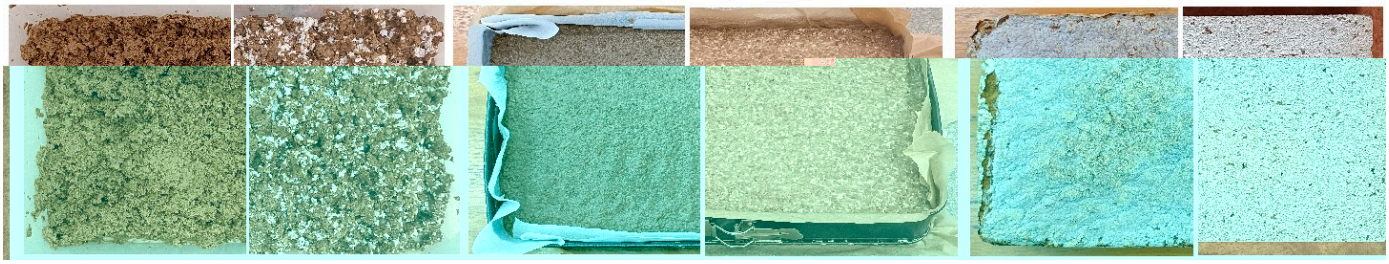

(a) (b) (c) (d) (e) (f)

Figure 1. Panel manufacturing phases: defibrated fibers via dry (**a**) and wet (**b**) techniques; prepared mixture for dry (**c**) and wet (**d**) method; composite panel before cutting (**e**); composite panel after cutting (**f**).

To ensure dimensional consistency and eliminate any overcooked or uneven surface layers, the panels were planed and cut to achieve uniform thickness (Figure 1e). For both wet and dry processing methods, four rectangular panels measuring 320 mm × 250 mm (length × width) were manufactured. After final trimming and surface preparation, the average thickness of each panel was reduced to 30 mm.

2.3. Vertical Density Profiles (VDPs) of the Samples

The VDPs of the resulting composites were determined using the IMAL X-ray density profiler DPX300 (San Damaso, Italy). Eight square specimens (50 mm × 50 mm) were cut from the panels for this purpose. Measurements were taken across the entire thickness of each specimen to assess the internal density distribution. Prior to profiling, each sample was weighed with a high-precision balance, model EU C-LCD made by Gibertini Elettronica (Novate Milanese, Italy). The analyzer's built-in measurement system was also used to confirm the sample dimensions, ensuring accurate density evaluation.

2.4. Affinity to Water

The absorption of water (WA) and the swelling in thickness (TS) were assessed according to the European standard SR EN 317:1996 [27] by immersing the specimens in distilled water. Five square specimens with nominal dimensions of 50 × 50 mm were sectioned from the experimental panels and subsequently subjected to a conditioning phase of 24 h at 20 ± 2 °C and 65 ± 5% relative humidity. The water absorption assessment was conducted in a controlled bath, wherein the specimens were fully submerged in distilled water maintained at 20 ± 1 °C for a duration of 24 h. Dimensional measurements were taken using a digital caliper with an accuracy of 0.01 mm. The mass of each sample was recorded at three specific intervals, namely before immersion, after 2 h, and after 24 h, employing an electronic balance with an accuracy of 0.01 g. The samples' thicknesses were measured at the central point along the diagonal of each specimen during every weighing phase to ensure consistency.

2.5. Thermal Conductivity Coefficient (λ) of the Samples

The thermal conductivity coefficient (λ) of the composite specimens was determined using a heat flow meter, model HFM436 Lambda made by Netzsch manufacturer from Selb, Germany. Two experimental composite configurations were tested in accordance with the guidelines of ISO 8301 [28] and DIN EN 12667 [29]. The sample was positioned between two flat plates, one that was heated up to 20 °C and the other that was cooled to as low as −10 °C, to measure the heat flux. The instrument calculated thermal conductivity automatically based on Fourier's Law, utilizing the temperature gradient between the plates. Before conducting the measurements, the system was calibrated following standard

protocols, which accounted for both the temperature difference (ΔT) and the average temperature (Tm) across the specimen (Table 2).

Table 2. Set parameters for the determination of λ.

Number of Tests	Temperature 1 Lower Plate	Temperature 2 Upper Plate	ΔT $T_2 - T_1$	Average $(T_1 + T_2)/2$
1	−10	20	30	5
2	−5	20	25	7.5
3	0	20	20	10
4	5	20	15	12.5
5	10	20	10	15
6	15	20	5	17.5

2.6. Sound Absorption Coefficient of the Samples

The sound absorption performance of the composite panels was evaluated across both low- and high-frequency ranges using impedance tube methods adapted to each frequency domain. To ensure accuracy and standardization, each method adhered to the relevant international testing standards.

2.6.1. Low-Frequency Sound Absorption Coefficient (α) Measurement

Low-frequency α-coefficient measurements were performed using a SCS80 FA impedance tube, from Vibro-Acoustic S.R.L. (Campodarsego PD, Italy), equipped with a two-microphone configuration. The procedure followed the guidelines of ISO 10534-2:1998 [30], which specifies the sound transfer method under normal incidence. α-coefficient was measured over a frequency range of 50 to 1390 Hz, with an incident sound pressure level of 75 dB.

For each type of composite, two specimens were tested. The maximum α-values for each specimen were calculated by the system's analysis software, and the average of these maximum values was used to assess the performance of the corresponding panel. This approach enabled effective comparison between the wet- and dry-processed composites within the low-frequency domain.

2.6.2. High-Frequency Sound Absorption Measurement

The high-frequency α-coefficient was evaluated using the impedance tube Brüel & Kjær (model 4206, Nærum, Denmark) based on the transfer function method with two microphones (TFM), in accordance with ISO 11654:1997, ISO 10534-2:1998, and ASTM E1050-12:1998 [30–32]. The measurements were performed under normal incidence conditions (0° angle) over a controlled frequency range of 100 Hz to 6400 Hz.

Each circular sample had a diameter of 29 mm and was tested using the sample holder of the impedance tube. Acoustic signals generated by the internal speaker were transmitted through the tube, and two microphones captured the responses. A data acquisition (DAQ) board and a signal conditioner processed and then analyzed the sound through a computer interface equipped with specialized acoustic analysis software.

To investigate the acoustic behavior of the samples under the effect of perforations, in addition to the standard wet- and dry-processed samples, modified versions of the same samples featuring seven uniformly distributed holes (each 3 mm in diameter) were also tested under identical conditions.

All measurements were conducted in a controlled laboratory environment, with ambient temperature of 22 ± 2 °C and 55 ± 5% relative humidity. This setup ensured repeatable and reliable characterization of the materials' sound absorption performance of the samples across the high-frequency spectrum.

2.7. Sample Porosity

The porosity volume of the specimens was measured using AccuPyc III 1350 Gas Pycnometer. For this analysis, five rectangular samples measuring 10 mm × 10 mm × 35 mm were prepared for each type. Precise dimensional measurements were obtained using a digital caliper with a resolution of 0.01 mm. The AccuPyc provides the true density (ρ_{true}) by displacing gas within the solid material, excluding interparticle voids but including closed pores. It also measures the bulk density (ρ_{bulk}) of the sample, accounting for pores and interparticle spaces. Porosity is calculated with Equation (1):

$$Porosity\ (\%) = \frac{\rho_{bulk}}{\rho_{true}} \cdot 100 \quad (1)$$

2.8. Microscopic Evaluation of the Samples

Stereo-microscopic observations were conducted using a Nikon SMZ18-LOT2 stereomicroscope manufactured by Nikon Corporation (Tokyo, Japan). This analysis facilitated the visual assessment and measurement of fiber dispersion, inter-fiber spacing, yeast incorporation within the composite matrix, and the integrity of fiber bonding. Images were acquired at a magnification of 120× on the two different composite types, selecting for this evaluation three samples cut from each composite.

2.9. Mechanical Properties of the Samples

Mechanical tests were conducted in accordance with applicable European standards, adhering to the specified procedures for sample preparation, including quantity, shape, and size. The MOE and MOR of the samples were measured by the universal testing machine Zwick/Roell Z010 (Ulm, Germany), with a loadcell with a capacity of 10,000 N, following the methodology described in EN 310:1993 [33]. Eight test specimens were prepared per composite type according to the specifications outlined in EN 326-1 [34].

IB strength, measured perpendicular to the panel surface, was evaluated according to EN 319 [35] using the Zwick/Roell Z010 testing system. For this test, eight square samples (50 mm × 50 mm) cut from each composite were examined.

2.10. Statistical Analysis

Statistical analyses were conducted to assess the significance of the differences between the composite groups. Standard deviations were calculated in Microsoft Excel, applying a 95% confidence interval with a significance threshold of $\alpha = 0.05$ ($p < 0.05$). To examine the effect of the two defibration techniques on the primary material properties, a two-sample *t*-test was performed using Minitab statistical software, version 19.2020.1. The analysis compared the mean values of the key parameters, including the vertical density profile, dimensional stability, thermal conductivity, MOE, MOR, and IB strength across the composite types.

3. Results and Discussion

The physical and mechanical properties of the samples are displayed in Table 3.

Table 3. Physical and mechanical properties of the samples.

Panel Type	Density (Kg/m^3)	WA (%)		TS (%)		λ (W/mK)	α_{max}	Porosity (%)	Flexural (N/mm^2)		IB (N/mm^2)
		2 h	24 h	2 h	24 h				MOE	MOR	
Wet	155.5	507.07	526.38	6.44	7.41	0.053	0.89	90	42.48	0.26	0.06
Dry	204.94	376.07	395.77	4.76	5.36	0.057	0.94	86.3	27.23	0.10	0.02

The performance of green lignocellulosic fiber-based insulation composites manufactured from recycled corrugated cardboard is fundamentally governed by the interplay between fiber morphology, degree of fibrillation, porosity, and gas expansion dynamics during the manufacturing process. Among these factors, the processing route, whether wet or dry, plays a decisive role in shaping the microstructural characteristics of the material, thereby exerting a direct influence on its physical, mechanical, thermal, and acoustic behavior. The choice of method is therefore not merely a processing decision but rather a key determinant of the functional performance and sustainability of the final product.

From a physical standpoint, the density and porosity of these composites are strongly dictated by the preparation method. Dry processing, typically involving hammer milling, produces coarser and less fibrillated fibers. These fibers exhibit reduced surface area and a more rigid morphology, which allows for denser packing during panel formation. As a result, the dry-processed composites generally attain a higher bulk density and lower void fraction. High porosity is obtained by accommodating enhanced gas retention and expansion when foaming agents, such as sodium bicarbonate and yeast, are activated during thermal treatment. The outcome is a foam-like, lightweight structure with improved open-cell architecture, reduced density, and the potential to optimize both thermal insulation and high-frequency acoustic absorption.

The degree of fibrillation achieved during wet processing holds particular significance. It increases the available surface area for hydrogen bonding between fibers and fines, thereby strengthening inter-fiber adhesion without relying on synthetic binders. Beyond simple adhesion, the fibrillated fibers act as reinforcement points within the matrix, distributing stress more uniformly and limiting crack initiation and propagation. Refining through wet processing further contributes to the regulation of pore size distribution, creating a more homogeneous structure that balances mechanical integrity with functional properties. Such improvements are directly reflected in mechanical indices, including flexural MOE, MOR, and IB strength. Composites characterized by finer fibers and uniform porosity are therefore anticipated to display superior stiffness, greater resistance to bending-induced fracture, and stronger cohesion through enhanced inter-fiber bonding.

The acoustic performance of these composites is similarly governed by the interaction between density and pore architecture. Panels with a higher density and compact structure typically exhibit improved absorption at lower frequencies, where mass-related damping and panel resonance dominate. On the other hand, higher-porosity panels with finely interconnected pore structures are more effective at attenuating high-frequency sound. This is achieved through viscous and thermal dissipation mechanisms occurring as sound waves penetrate the pore network. The balance between these two behaviors highlights a unique opportunity for design flexibility; by adjusting processing parameters and pore structure, cardboard-based composites can be tuned to target either low-frequency or high-frequency sound absorption or engineered to perform across a wider frequency range. Additional structural modifications, such as controlled surface perforation, may further expand the acoustic response, potentially enabling nearly total absorption at certain frequencies, which is a characteristic highly desirable for architectural and industrial noise-control applications.

Thermal conductivity, a key criterion for insulation materials, is closely correlated with density and porosity. Lower-density composites with higher void fractions contain a larger proportion of entrapped air, which functions as an efficient thermal barrier and minimizes heat transfer. Conversely, higher-density composites, while offering enhanced mechanical stability, facilitate greater solid-phase conduction pathways, thereby raising thermal conductivity. However, once their porosity exceeds 80%, the differences in density or porosity have only a minor influence on thermal conductivity, since heat transfer occurs mainly through stagnant air rather than the solid matrix.

From the perspective of sustainable material engineering, these interrelationships highlight a critical opportunity to tailor recycled cardboard-based insulation products to diverse functional applications without the need for synthetic polymers, formaldehyde-based adhesives, or energy-intensive binders. This advantage directly supports global efforts to reduce dependency on petroleum-derived construction materials while aligning with circular economy principles. Wet processing, owing to its ability to generate lightweight, mechanically resilient, and acoustically efficient panels, can be prioritized for applications emphasizing energy efficiency and sound management in building envelopes. In contrast, dry processing offers value in contexts requiring mass-related damping or enhanced low-frequency acoustic response, where the trade-off of higher density may be beneficial.

Equally important, the utilization of recycled corrugated cardboard as a feedstock confers significant environmental benefits. With global cardboard recycling rates already approaching 90%, redirecting this abundant post-consumer resource into high-value insulation products extends its lifecycle and mitigates the environmental burdens of landfilling or incineration. Moreover, integrating foaming and leavening agents, such as sodium bicarbonate and yeast, introduces a low-energy, non-toxic manufacturing pathway that avoids the challenges of conventional insulation production, such as high embodied energy, poor biodegradability, and hazardous emissions.

All in all, the influence of fiber morphology, processing method, and pore architecture demonstrates the versatility of green lignocellulosic fiber-based composites in advancing sustainable construction materials. By leveraging simple yet effective manufacturing strategies, it becomes possible to design insulation products with tailored combinations of mechanical, thermal, and acoustic performance, thereby offering viable, biodegradable alternatives to conventional inorganic and synthetic insulations widely used in the construction sector. A summary of the statistics for the measured properties of the samples is shown in Table 4.

Table 4. Statistical significance of the measured properties of the samples.

Property	Wet (Mean ± SD)	Dry (Mean ± SD)	*p*-Value	Significance
Density (Kg/m^3)	155.5 ± 13.83	204.94 ± 8.70	0.000	Significant
WA 2 h (%)	507.07 ± 95	376.07 ± 38	0.132	Not Significant
WA 24 h (%)	526.38 ± 91	395.77 ± 41	0.055	Not Significant
TS 2 h (%)	6.44 ± 0.5	4.76 ± 0.4	0.010	Significant
TS 24 h (%)	7.41 ± 0.5	5.36 ± 0.4	0.024	Significant
λ (W/mK)	0.053 ± 0.001	0.057 ± 0.003	0.048	Significant
MOE (N/mm^2)	42.48 ± 2	27.23 ± 3	0.000	Significant
MOR (N/mm^2)	0.26 ± 0.01	0.10 ± 0.02	0.000	Significant
IB (N/mm^2)	0.06 ± 0.005	0.02 ± 0.005	0.001	Significant

3.1. Vertical Density Profiles (VDPs) of the Samples

The VDPs of the panels made using the wet and dry processing methods exhibited distinct differences reflecting the influence of manufacturing conditions on panel compaction and internal structure. The dry-processed panel demonstrated a significantly higher average density of 204.94 kg/m^3, whereas the wet-processed panel showed a relatively lower density of 155.5 kg/m^3. Statistical analysis has shown that this difference was significant ($p < 0.05$), indicating a strong influence of the processing method on the bulk density of the panels.

This variation can be primarily attributed to differences in fiber morphology [20] and gas expansion behavior [36,37] during processing rather than compaction efficiency. The dry-processed fibers, obtained from the hammer mill, were coarser and less fibrillated, enabling denser packing and reducing void formation, which is consistent with the lower porosity value of 86.3%.

In contrast, the wet-processed fibers, prepared with a blender, underwent significant fibrillation and water-induced swelling, promoting a looser fiber network. Additionally, the water-induced swelling likely enhanced CO_2 evolution from the sodium bicarbonate and yeast system during baking, generating a more foamed structure. Consequently, the wet-processed panel exhibited a markedly higher porosity (90%), resulting in a 24% lower bulk density compared to its dry-processed counterpart.

The VDP curves in Figure 2 further illustrate the density distribution across the panel thickness for both processing methods. The wet-processed panel in Figure 2a also exhibited a more irregular density profile, characterized by a lower and relatively uniform core density with a value of ~155 kg/m^3. The smoother transition from surface to core density indicates an integrated structure, consistent with the higher porosity and greater water absorption behavior observed for this panel.

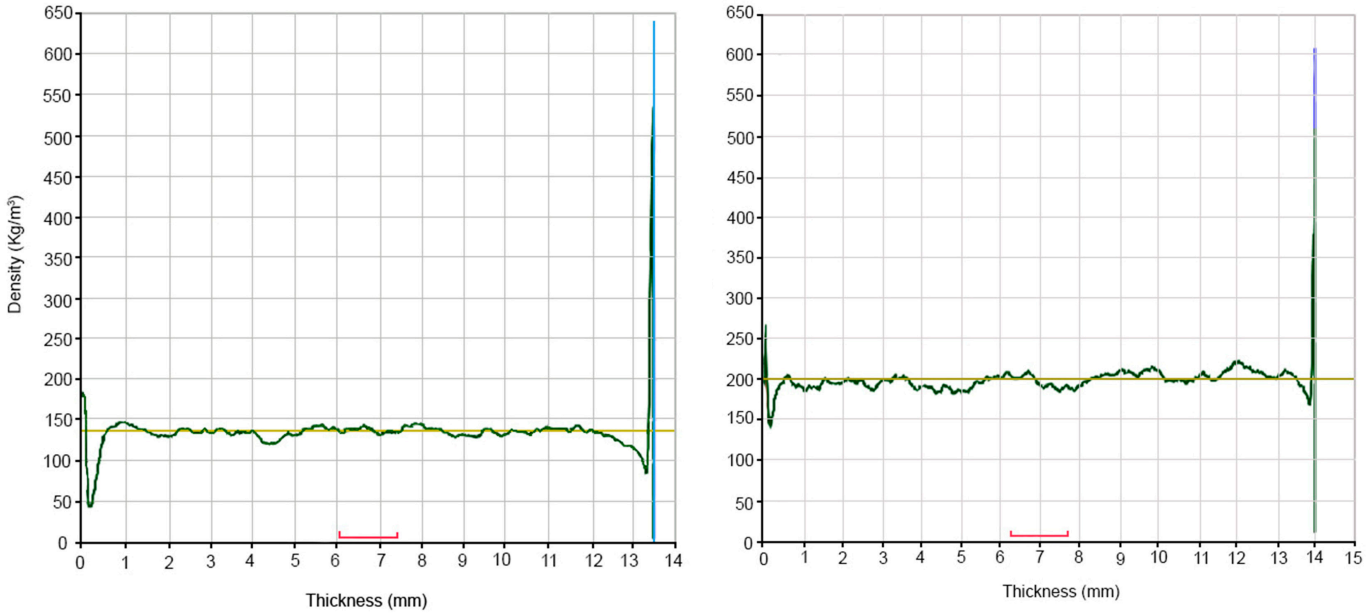

(**a**) (**b**)

Figure 2. Typical vertical density profiles of the wet-processed (**a**) and dry-processed (**b**) samples.

In contrast, the dry-processed panels shown in Figure 2b exhibited a relatively stable density profile, maintaining values close to the average of ~205 kg/m^3 across the core region, with slight fluctuations between 180 and 220 kg/m^3.

3.2. Water Affinity of the Composites

The affinity to water, evaluated in terms of water absorption and thickness swelling, exhibited significant differences between the wet- and dry-processed composites ($p < 0.05$ for TS; $p > 0.05$ for WA), as illustrated in Figure 3. The wet-processed panel demonstrated markedly higher water absorption values, reaching 507.07% after 2 h and increasing slightly to 526.38% after 24 h. In contrast, the dry-processed panel absorbed substantially less water, with water absorption values of 376.07% and 395.77% after 2 and 24 h, respectively. However, the differences in water absorption between the two panels were not statistically significant, with $p > 0.05$, group A in Figure 3. This pronounced difference can be attributed to the greater porosity and open-cell structure of the wet-processed panel, with 90% porosity compared to the corresponding value of 86.3% for the denser and more compact dry-processed samples. The highly fibrillated and water-swollen fibers generated during wet processing likely created interconnected voids, promoting rapid water penetration and

retention, whereas the coarser, less fibrillated fibers of the dry-processed panel contributed to reduced capillary water uptake.

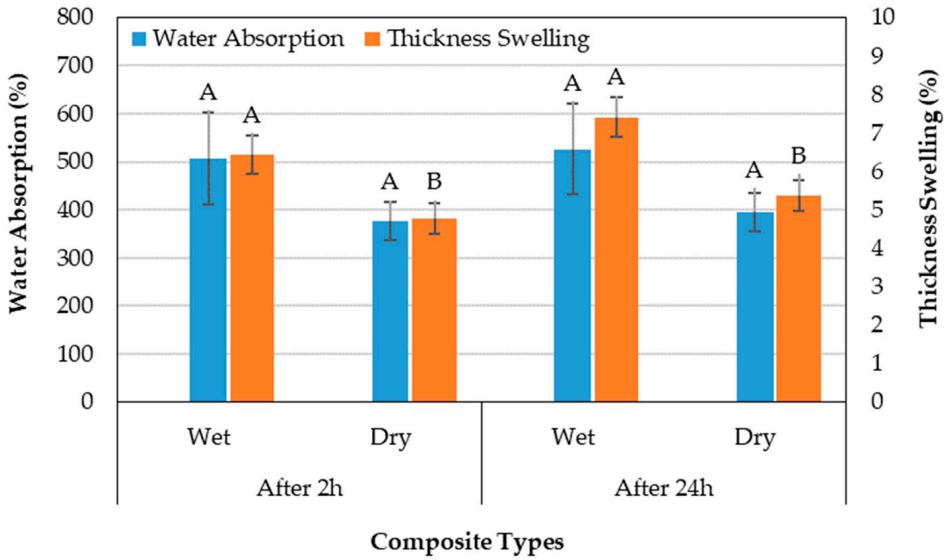

Figure 3. WA and TS after 2 h and 24 h of water immersion.

Similarly, TS followed the same trend, with the wet-processed panel exhibiting higher swelling values of 6.44% after 2 h and 7.41% after 24 h, compared to 4.76% and 5.36% for the dry-processed panel for the same time intervals. Unlike water absorption, the differences in TS were statistically significant at both time intervals, with $p < 0.05$, (groups A and B). The greater thickness swelling in the wet-processed panel is consistent with its higher water absorption and its less consolidated fiber network, which undergoes more significant expansion when saturated. The dry-processed panel, with its denser internal structure, exhibited better resistance to swelling, highlighting its superior dimensional stability under humid conditions.

These findings indicate that while the wet-processed panel may offer potential advantages for applications where low density and high porosity are desirable (e.g., thermal or acoustic insulation), its poor dimensional stability limits its suitability for structural or load-bearing applications. In contrast, the dry-processed panel demonstrates better dimensional stability, making it more appropriate for applications requiring improved resistance to moisture-induced deformation.

3.3. Thermal Conductivity Coefficient (λ) of the Samples

The panels exhibited a significant difference between the wet- and dry-processed composites ($p < 0.05$) in terms of λ-values, highlighting the influence of processing method and resulting microstructural characteristics on the heat transfer behavior, as shown in Figure 4. The wet-processed panels demonstrated a lower thermal conductivity value of 0.053 W/mK, whereas the dry-processed panel had a λ value of 0.057 W/mK. Although this absolute difference appears small, it is statistically meaningful (groups A and B) and consistent with the distinct structural features of the two panels.

The lower λ-value of the wet-processed panel can be attributed to its higher porosity (90%) and lower bulk density (155.5 kg/m^3), which are consequences of extensive fiber fibrillation and gas expansion during wet processing. The open, foam-like structure likely entrapped more air within the panel matrix, and since air is a poor thermal conductor, this resulted in reduced heat transfer. Conversely, the dry-processed panel, with its denser fiber packing (204.94 kg/m^3) and lower porosity (86.3%), provided increased solid–solid contact

between fibers, enhancing conduction pathways and thus increasing thermal conductivity. A direct relationship between density and thermal conductivity has been consistently documented in previous research [1,38], underscoring the critical role that bulk density plays in governing heat transfer behavior within lignocellulosic composites. However, both panels are highly porous, and the dominant contributor to thermal insulation is still the entrapped air phase, which has very low thermal conductivity (0.025 W/mK). In such low-density composites, once the porosity exceeds 80%, further changes in density or porosity have only a minor influence on thermal conductivity, since heat transfer occurs mainly through the entrapped air, rather than the solid matrix [39]. Several researchers have emphasized that thermal transport in porous media is largely dictated by the characteristics of the pore network. In agreement with this, Clarke [40] reported that the decrease in thermal conductivity is critically influenced by the pore volume fraction, the aspect ratio, and the spatial distribution of the pores. Other properties, such as mechanical strength and water absorption, are more strongly influenced by these structural differences.

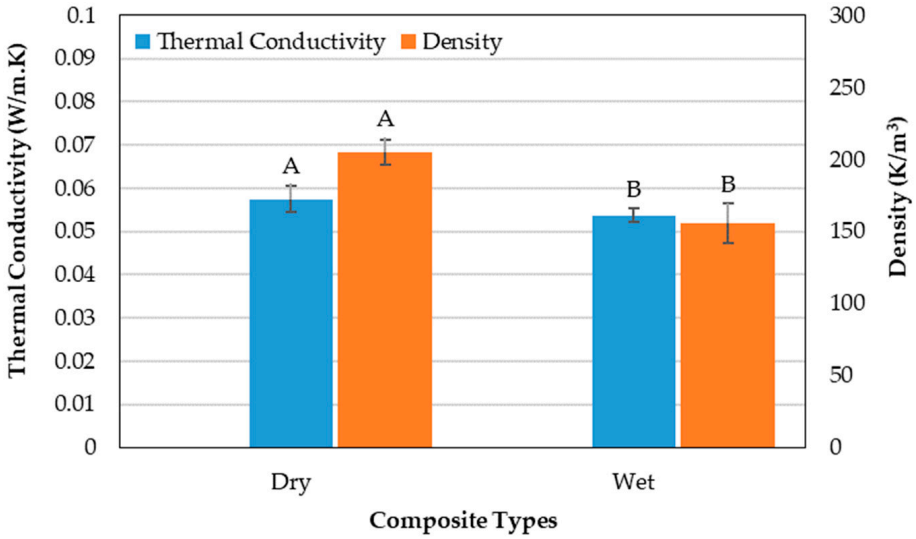

Figure 4. Thermal conductivity coefficient versus density of the samples.

These findings suggest that the wet-processed panel, due to its superior thermal insulation capability, may be more suitable for non-structural applications, such as thermal or acoustic insulation. In contrast, the dry-processed panel, despite its slightly higher thermal conductivity, is more appropriate for applications requiring enhanced mechanical performance and dimensional stability.

3.4. Sound Absorption Coefficient (α) of the Samples

The sound transfer through the panels was evaluated over both low-frequency (50–1390 Hz) and high-frequency (100–6400 Hz) domains, revealing distinct effects of processing method and panel configuration on acoustic performance.

In the low-frequency range (Figure 5), both panels exhibited high sound absorption potential, with the dry-processed panel slightly outperforming the wet-processed one. Specifically, the dry-processed panel achieved a maximum sound absorption coefficient (α_{max}) of 0.94, compared to 0.89 for the wet-processed panel at 700 Hz frequency. Despite the wet-processed panel's higher porosity and fibrillated structure, the more compact structure of the dry-processed panel appears to favor the dissipation of low-frequency acoustic waves, potentially due to better impedance matching with the surrounding air.

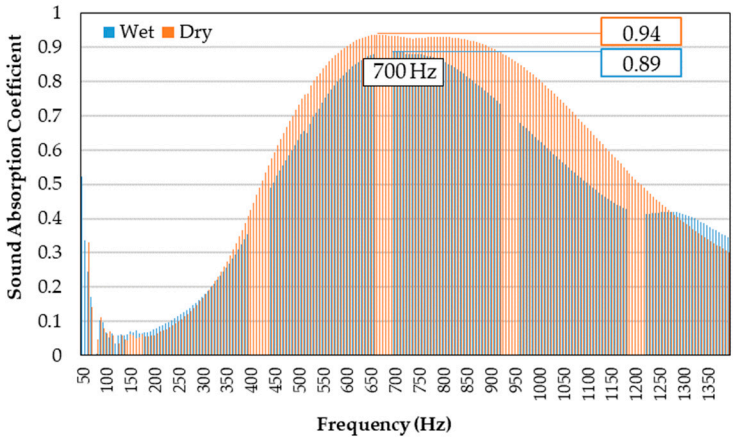

Figure 5. α-coefficient of the samples (measured for low-frequency range).

In the high-frequency range (Figure 6), the results indicated a clear advantage for the wet-processed panels, especially when modified with perforations. Among the unperforated samples, the wet-processed panel recorded an α_{max} of 0.84, outperforming the dry-processed counterpart, which reached 0.75. This enhancement is attributed to the highly porous and interconnected fiber network of the wet-processed composite, which promotes efficient absorption through viscous losses and internal friction mechanisms [41].

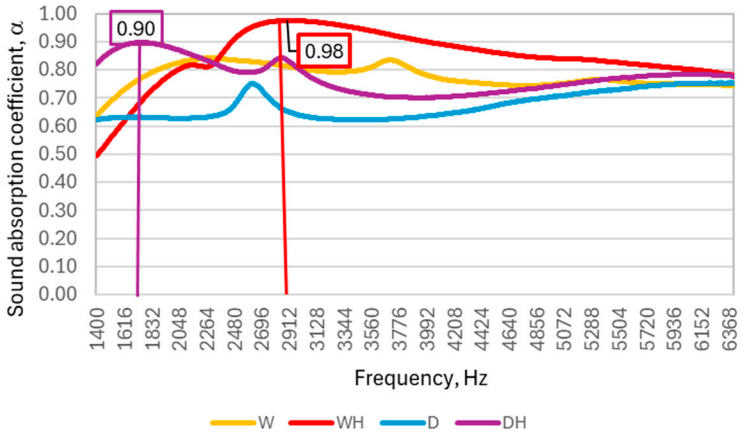

Figure 6. α-coefficient of the samples (measured for high-frequency range).

When perforations were introduced, sound absorption performance improved significantly for both processing methods. The wet-processed panel with holes had an α_{max} of 0.98, the highest among all the samples, while the dry-processed panel with holes reached 0.90. The presence of perforations likely facilitates multiple acoustic wave reflections and longer travel paths within the panel matrix, amplifying energy dissipation. The combination of wet processing and structural perforation proved particularly effective, suggesting a strong synergistic effect between fiber morphology and design optimization. Composite density is influenced by substrate choice, processing method, and post-treatment [42]. Foam layer performance improves with higher pore density and contact area achieved through optimized geometry, finer fibrils, and controlled density [42]. Resonance tuning is possible by adjusting thickness and perforation design, including cavity number, size, depth, and distribution [43].

These findings demonstrate that both material processing and structural modification have a substantial influence on acoustic behavior. While the dry-processed panel offered slightly better low-frequency absorption, wet-processed panels, especially with

perforations, exhibited superior broadband sound absorption, making them well-suited for applications requiring effective acoustic damping across a wide frequency spectrum.

3.5. Mechanical Behavior of the Samples

The performance of the composite panels (Figure 7) was assessed through measurements of flexural MOE, MOR, and IB strength. All three properties of the wet- and dry-processed panels exhibited statistically significant differences ($p < 0.05$) between them (different groups A and B), indicating that the processing method plays a pivotal role in determining their mechanical performance.

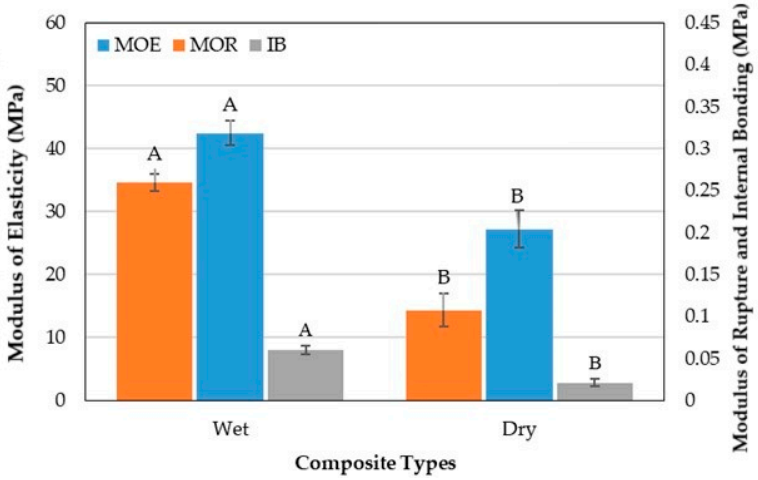

Figure 7. Mechanical properties of the samples.

The wet-processed panel demonstrated a superior MOE of 42.48 MPa, significantly higher than the 27.23 MPa observed for the dry-processed panel. This 36% increase in stiffness is attributed to the finer, more fibrillated fibers generated during the wet process, which likely created more extensive fiber–fiber contact areas and improved stress transfer within the composite matrix.

Similarly, the MOR of the wet-processed panel reached 0.26 MPa, more than double that of the dry-processed panel, with a value of 0.10 MPa, reflecting its greater resistance to failure for 61% under bending stress. The increased MOR further supports the hypothesis that the wet processing method leads to a better-integrated fiber network with improved structural cohesion.

Internal bonding strength followed the same trend. The wet-processed panel achieved a value of 0.06 N/mm^2, compared to 0.02 MPa for the dry-processed sample. This substantial difference (67%) may result from the improved fiber surface area and bonding potential induced by mechanical fibrillation in the wet processing stage, which promotes stronger inter-fiber adhesion during thermal cooking.

These improvements are primarily attributed to the finer, more fibrillated fibers produced during wet processing, which increase fiber–fiber contact areas, facilitating stress transfer within the composite matrix, and enabling additional hydrogen bonds between fibers and fines. Furthermore, the refining effect inherent to wet processing can regulate and control foam microstructure, leading to more uniform stress distribution and enhanced load-bearing capacity. Such synergistic effects of fiber morphology modification and microstructural optimization provide a clear mechanistic basis for the superior mechanical performance of wet-processed panels [20].

Collectively, these results indicate that the wet processing method produces composite panels with significantly enhanced mechanical properties, suggesting its potential for use in applications where flexural strength and internal cohesion are critical. In contrast, the

lower mechanical performance of the dry-processed panels may limit their suitability for structural uses, but they could be acceptable in applications where the mechanical demands are less stringent.

3.6. Microscopic Evaluation of the Samples

A microscopic investigation was conducted using stereo-microscopy at a magnification of 120× to evaluate the morphological characteristics of fibers within the composite structure, providing insight into how processing methods influenced fiber dispersion and surface texture (Figure 8). The dry-processed composite (Figure 8a) revealed a network of coarser fibers with minimal fibrillation and relatively smooth surfaces. The fiber diameters ranged from approximately 15.38 µm to 42.28 µm, with most fibers appearing intact and less mechanically degraded. This morphology is indicative of the hammer milling process used in dry preparation, which preserves the structural integrity of the fibers but limits surface area exposure and matrix interlocking. The observed compact fiber arrangement is consistent with the lower porosity (86.3%) and higher density (204.94 kg/m^3) measured for the dry-processed panels.

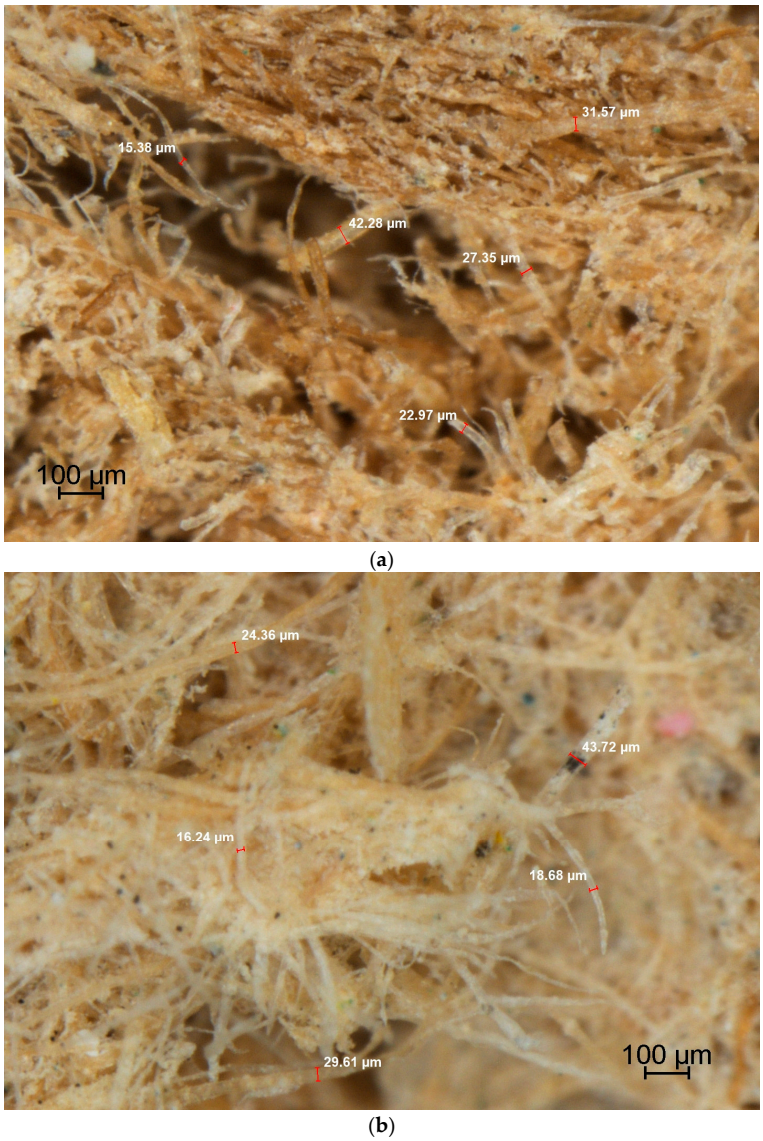

Figure 8. Microscopic investigation of the samples at 120× magnification; (**a**) dry-processed composite; (**b**) wet-processed composite.

In contrast, the wet-processed composite (Figure 8b) exhibited a markedly different microstructure. The fibers were significantly more fibrillated and entangled, with finer elements distributed throughout the matrix. Fiber diameters ranged from 16.24 μm to 43.72 μm, but many fibers appeared fragmented, with frayed ends and delaminated surfaces. These features are a direct result of the high-shear blending and water-induced swelling that occur during wet processing. The enhanced fibrillation leads to an open and more porous network, in line with the measured porosity of 90% and reduced density (155.5 kg/m^3) for the wet-processed panels. Moreover, this loose fiber architecture is believed to facilitate greater gas expansion during foaming and higher water absorption due to increased capillary pathways.

These microstructural features are consistent with the superior mechanical performance observed for the wet-processed panel. These substantial improvements are attributed to enhanced fibrillation, increased fiber surface area, and stronger inter-fiber bonding potential resulting from the wet processing method. Statistical analysis of the mechanical properties confirmed that these differences were significant ($p < 0.05$), further supporting the positive influence of fiber morphology and microstructural refinement on the mechanical behavior of binder-less fiber composites.

4. Conclusions

This study comprehensively investigated the influence of wet and dry processing techniques on the structural, physical, mechanical, thermal, and acoustic performance of binder-less natural fiber composites. The results clearly indicate that the processing method plays a pivotal role in defining the internal microstructure and, consequently, the overall behavior of the panels across multiple performance domains.

The dry-processed panels with a higher density value of 204.94 kg/m^3 and lower porosity value of 86.3% demonstrated superior dimensional stability, particularly in terms of their thickness swelling. Although the water absorption differences between the two methods were not statistically significant from each other, the dry-processed samples maintained better structural integrity under moisture exposure. In the case of thermal conductivity, the wet-processed panel showed a significantly lower thermal conductivity value of 0.053 W/mK versus 0.057 W/mK for the dry samples, reflecting enhanced insulation performance due to its more porous internal architecture.

Contrary to expectations based on their lower density, the wet-processed panels exhibited superior mechanical properties, achieving statistically significant increases in MOE, MOR, and IB strength compared to the dry-processed panel. Such enhancement could be attributed to improved and homogeneous fibrillation and inter-fiber bonding facilitated by the wet processing method. Microscopic examination supported these observations, revealing a more compact, homogeneous, and well-bonded fiber network in the wet-processed panel, while the dry-processed composite appeared to be more heterogeneous, with poorly integrated fiber bundles and voids. These microstructural differences can also be directly contributed to the observed variation in mechanical strength of the samples.

The acoustic performance of the panels further highlighted the nuanced impact of processing methods. In the low-frequency range (50–1390 Hz), the dry-processed panel achieved a slightly higher maximum sound absorption coefficient, with α_max reaching 0.94, compared to 0.89 for the wet-processed sample. However, in the high-frequency range (100–6400 Hz), the wet-processed panel outperformed its dry counterpart, with α_max recorded at 0.84 versus 0.75. The perforations with seven holes and 3 mm diameter in both panel types further enhanced the overall high-frequency absorption, with the wet-processed perforated panels attaining an α_max of 0.98, while the dry-processed perforated

panels reached 0.90. These results emphasize the potential of structural modifications to improve acoustic performance and tailor composites for targeted frequency ranges.

In conclusion, wet processing, despite yielding composites with lower dimensional stability, resulted in materials with improved mechanical strength, thermal insulation, and high-frequency sound absorption capabilities. Conversely, dry processing favored dimensional stability and low-frequency acoustic performance. These findings offer valuable insights for engineering multifunctional, eco-friendly composites and demonstrate how processing routes can be chosen strategically to meet the diverse requirements of applications in building materials, acoustic insulation, and sustainable construction systems.

Author Contributions: Conceptualization, M.H.M. and C.C.; methodology, C.C. and S.H.; software, L.M.B.; validation, C.C., S.H., and L.M.B.; formal analysis, S.H.; investigation, M.H.M.; resources, M.H.M.; data curation, C.C.; writing—original draft preparation, M.H.M.; writing—review and editing, S.H. and C.C.; visualization, L.M.B.; supervision, S.H., C.C., and L.M.B.; project administration, C.C.; funding acquisition, M.H.M. All authors have read and agreed to the published version of the manuscript.

Funding: This research received no external funding.

Institutional Review Board Statement: Not applicable.

Informed Consent Statement: Not applicable.

Data Availability Statement: Data are contained within the article.

Conflicts of Interest: The authors declare no conflicts of interest.

References

1. Mathews, J.M.; Vivek, B.; Charde, M. Thermal insulation panels for buildings using recycled cardboard: Experimental characterization and optimum selection. *Energy Build.* **2023**, *281*, 112747. [CrossRef]
2. Bi, L.J. Research on corrugated cardboard and its application. *Adv. Mater. Res.* **2012**, *535*, 2171–2176. [CrossRef]
3. Lohtander, T.; Herrala, R.; Laaksonen, P.; Franssila, S.; Österberg, M. Lightweight lignocellulosic foams for thermal insulation. *Cellulose* **2022**, *29*, 1855–1871. [CrossRef]
4. Antunes, M.D.S.P.; Cano, Á.; Realinho, V.C.D.R.; Osuna, D.A.; Perero, J.I.V. Compression properties and cellular structure of polyurethane composite foams combining nanoclay and different reinforcements. *Int. J. Compos. Mater.* **2014**, *4*, 27–34.
5. Kausar, A. Polyurethane composite foams in high-performance applications: A review. *Polym.-Plast. Technol. Eng.* **2018**, *57*, 346–369. [CrossRef]
6. Yucel, K.; Basyigit, C.; Ozel, C. Thermal insulation properties of expanded polystyrene as construction and insulating materials. In Proceedings of the 15th Symposium in Thermophysical Properties, Boulder, CO, USA, 22–27 June 2003.
7. Benallel, A.; Tilioua, A.; Ettakni, M.; Ouakarrouch, M.; Garoum, M.; Hamdi, M.A.A. Design and thermophysical characterization of new thermal insulation panels based on cardboard waste and vegetable fibers. *Sustain. Energy Technol. Assess.* **2021**, *48*, 101639. [CrossRef]
8. Benallel, A.; Tilioua, A.; Mellaikhafi, A.; Babaoui, A.; Hamdi, M.A.A. Thermal characterization of insulating materials based on date palm particles and cardboard waste for use in thermal insulation building. In Proceedings of the AIP Conference Proceedings, Virtual, 26–28 April 2021; AIP Publishing: Melville, NY, USA, 2021; Volume 2345, p. 020024.
9. Cintura, E.; Nunes, L.; Esteves, B.; Faria, P. Agro-industrial wastes as building insulation materials: A review and challenges for Euro-Mediterranean countries. *Ind. Crops Prod.* **2021**, *171*, 113833. [CrossRef]
10. Xie, M.; Qiao, Q.; Sun, Q.; Zhang, L. Life cycle assessment of composite packaging waste management—A Chinese case study on aseptic packaging. *Int. J. Life Cycle Assess.* **2013**, *18*, 626–635. [CrossRef]
11. FAO. *World Production Cardboard*; Food and Agriculture Organization: Rome, Italy, 2021.
12. Mazaherifar, M.H.; Coşereanu, C.; Timar, C.M.; Georgescu, S.V. Physical and mechanical properties of foam-type panels manufactured from recycled cardboard. *Constr. Build. Mater.* **2024**, *411*, 134685. [CrossRef]
13. Miller, M.; Justiniano, M.; McQueen, S. *Energy and Environmental Profile of the US Pulp and Paper Industry*; Energetics, Inc.: Columbia, MD, USA, 2005.
14. Virtanen, Y.; Nilsson, S. *Environmental Impacts of Waste Paper Recycling*; Routledge: Abingdon, UK, 2013.

15. Mahdi, S.; Xie, T.; Venkatesan, S.; Gravina, R.J. Mechanical characterisation and small-scale life-cycle assessment of polypropylene macro-fibre blended recycled cardboard concrete. *Constr. Build. Mater.* **2023**, *409*, 133902. [CrossRef]
16. Betts, D.; Sadeghian, P.; Fam, A. Structural behavior of sandwich beams with flax fiber–reinforced polymer faces and cardboard cores under monotonic and impact loads. *J. Archit. Eng.* **2020**, *26*, 04020013. [CrossRef]
17. McCracken, A.; Sadeghian, P. Corrugated cardboard core sandwich beams with bio-based flax fiber composite skins. *J. Build. Eng.* **2018**, *20*, 114–122. [CrossRef]
18. Sair, S.; Mandili, B.; Taqi, M.; El Bouari, A. Development of a new eco-friendly composite material based on gypsum reinforced with a mixture of cork fibre and cardboard waste for building thermal insulation. *Compos. Commun.* **2019**, *16*, 20–24. [CrossRef]
19. Mazaherifar, M.H.; Timar, M.C.; Georgescu, S.V.; Coșereanu, C. Sustainable thermal and acoustic insulating panels from recycled cardboard. *BioResources* **2025**, *20*, 4115–4135. [CrossRef]
20. Li, J.; Yang, X.; Xiu, H.; Dong, H.; Song, T.; Ma, F.; Ji, Y. Structure and performance control of plant fiber based foam material by fibrillation via refining treatment. *Ind. Crops Prod.* **2019**, *128*, 186–193. [CrossRef]
21. Liuzzi, S.; Rubino, C.; Martellotta, F.; Stefanizzi, P. Sustainable Materials from Waste Paper: Thermal and Acoustical Characterization. *Appl. Sci.* **2023**, *13*, 4710. [CrossRef]
22. Woodhams, R.; Thomas, G.; Rodgers, D. Wood fibers as reinforcing fillers for polyolefins. *Polym. Eng. Sci.* **1984**, *24*, 1166–1171. [CrossRef]
23. Nair, A.S.; Al-Battashi, H.; Al-Akzawi, A.; Annamalai, N.; Gujarathi, A.; Al-Bahry, S.; Sivakumar, N. Waste office paper: A potential feedstock for cellulase production by a novel strain Bacillus velezensis ASN1. *Waste Manag.* **2018**, *79*, 491–500. [CrossRef]
24. Xu, H.; Huang, L.; Xu, M.; Qi, M.; Yi, T.; Mo, Q.; Zhao, H.; Huang, C.; Wang, S.; Liu, Y. Preparation and properties of cellulose-based films regenerated from waste corrugated cardboards using [Amim] Cl/$CaCl_2$. *ACS Omega* **2020**, *5*, 23743–23754. [CrossRef] [PubMed]
25. Chinga-Carrasco, G. Cellulose fibres, nanofibrils and microfibrils: The morphological sequence of MFC components from a plant physiology and fibre technology point of view. *Nanoscale Res. Lett.* **2011**, *6*, 417. [CrossRef]
26. Wang, X.; Sotoudehniakarani, F.; Yu, Z.; Morrell, J.J.; Cappellazzi, J.; McDonald, A.G. Evaluation of corrugated cardboard biochar as reinforcing fiber on properties, biodegradability and weatherability of wood–plastic composites. *Polym. Degrad. Stab.* **2019**, *168*, 108955. [CrossRef]
27. *EN 317:1996*; Particleboards and Fibreboards—Determination of Swelling in Thickness after Immersion in Water. European Committee for Standardization: Brussels, Belgium, 1996.
28. *ISO 8301:1991*; Determination of Steady-State Thermal Resistance and Related Properties. Heat Flow Meter Apparatus. International Organization for Standardization: Geneva, Switzerland, 1991.
29. *BS EN 12939:2001*; Thermal Performance of Building Materials and Products: Determination of Thermal Resistance by Means of Guarded Hot Plate and Heat Flow Meter Methods: Products of High and Medium Thermal Resistance. British Standards Institution: London, UK, 2001.
30. *ISO 10534:1998*; Acoustics—Determination of Sound Absorption Coefficient and Impedance in Impedance Tubes: Part 1: Method Using Standing Wave Ratio. Part 2: Transfer-Function Method. International Organization for Standardization: Geneva, Switzerland, 1998.
31. *ASTM E1050:1998*; Standard Test Method for Impedance and Absorption of Acoustical Materials Using a Tube, Two Microphones and a Digital Frequency Analysis System. ASTM International: West Conshohocken, PA, USA, 1998.
32. *ISO 11654:1997*; Acoustics: Sound Absorbers for Use in Buildings. Rating of Sound Absorption. International Organization for Standardization: Geneva, Switzerland, 1997.
33. *EN 310:1993*; Wood-Based Panels—Determination of Modulus of Elasticity in Bending and of Bending Strength. European Committee for Standardization: Brussels, Belgium, 1993.
34. *EN 326-1:1994*; Wood-Based Panels. Sampling, Cutting and Inspection. Part 1: Sampling and Cutting of Test Pieces and Expression of Test. European Committee for Standardization: Brussels, Belgium, 1994.
35. *EN 319:1993*; Particleboards and Fibreboards: Determination of Tensile Strength Perpendicular to the Plane of the Board. European Committee for Standardization: Brussels, Belgium, 1993.
36. Fauzi, M.S.; Lan, D.N.; Osman, H.; Ghani, S.A. Effect of sodium bicarbonate as blowing agent on production of epoxy shape memory foam using aqueous processing method. *Sains Malays.* **2015**, *44*, 869–874. [CrossRef]
37. Hussein, M.S.; Leng, T.P.; Rahmat, A.R.; Zainuddin, F.; Keat, Y.C.; Suppiah, K.; Alsagayar, Z.S. The effect of sodium bicarbonate as blowing agent on the mechanical properties of epoxy. *Mater. Today Proc.* **2019**, *16*, 1622–1629. [CrossRef]
38. Benallel, A.; Tilioua, A.; Garoum, M. Development of thermal insulation panels bio-composite containing cardboard and date palm fibers. *J. Clean. Prod.* **2024**, *434*, 139995. [CrossRef]
39. Janssen, H.; Van De Walle, W. The impact of pore structure parameters on the thermal conductivity of porous building blocks. *Constr. Build. Mater.* **2022**, *324*, 126681. [CrossRef]

40. Clarke, D.R. Materials selection guidelines for low thermal conductivity thermal barrier coatings. *Surf. Coat. Technol.* **2003**, *163–164*, 67–74. [CrossRef]
41. Gokulkumar, S.; Thyla, P.R.; Prabhu, L.; Sathish, S. Measuring methods of acoustic properties and influence of physical parameters on natural fibers: A review. *J. Nat. Fibers* **2020**, *17*, 1719–1738. [CrossRef]
42. Mamtaz, H.; Fouladi, M.H.; Al-Atabi, M.; Namasivayam, S.N. Acoustic Absorption of Natural Fiber Composites. *J. Eng.* **2016**, e5836107. [CrossRef]
43. Sun, W.; Strässle Zúñiga, S.H.; Philippe, V.; Rinaldi, L.; Abitbol, T. Mycelium-Bound composites from agro-industrial waste for broadband acoustic absorption. *Mater. Des.* **2025**, *250*, 113591. [CrossRef]